Coherent electronic transport and Kondo resonance in magnetic nanostructures

Bogdan R. Bułka and Stanisław Lipiński
Institute of Molecular Physics, Polish Academy of Sciences,
M. Smoluchowskiego 17, 60-179 Poznań, Poland

(Dated: October 14, 2002)

Abstract

We consider coherent electronic transport between two ferromagnetic electrodes separated either by a metallic nanoparticle or by a conducting molecule. Correlations between electrons with opposite spins lead to the Kondo resonance, which manifests a formation of the singlet state. Although tunnelling rates for electrons with opposite spin orientations are different the conductance reaches the unitary limit in the Kondo regime. We predict a negative magnetoresistance effect, which can be observed for asymmetric magnetic junctions.

PACS numbers: 73.63.-b,72.20.My, 85.75.Mm

I. INTRODUCTION

Spin-dependent electronic transport attracts recently great interest due to its potential applications in nanoelectronics. In the last decade intensive studies of giant magnetoresistance (GMR) led to a practical application of the effect in magnetic field sensors and read heads for drives.[1] More recent studies of tunnel magnetoresistance (TMR) in multilayered metal-nonmetal thin films or in metal-nonmetal granular systems seem also to be very promising.[2] An interesting proposition is a ferromagnetic single–electron transistor (fSET)[3,4], in which transport through a nanoparticle placed between ferromagnetic electrodes is a single-electron process. Due to high contact resistances ($R > 10\mathrm{M}\Omega$) the current intensity is, however, very low and tunnelling events for transfer of an electron to and from the nanoparticle are incoherent. One can expect that further development in technology leads to a production of magnetic nanodevices operating in the coherent regime of the electronic transport. This is achieved if a typical dimension of the object becomes smaller than the phase coherence length. The issue of coherence is critical for the possible application in quantum computers.

There are known experiments on coherent transport in nonmagnetic nanostructures, through quantum dots[5] and single-walled carbon nanotubes (SWNT)[6]. In this regime quantum interference and electronic correlations play an essential role, they lead to the Fano resonance as well as to the Kondo resonance.[5–7] The coherence effects should be also important in magnetic nanostructures. Garcia et al. [8] showed that the relative difference between the resistance for the parallel (R_P) and the antiparallel (R_{AP}) orientation of magnetization in the electrodes $MR = (R_{AP} - R_P)/R_{AP}$ can be very large in the ballistic transport through a magnetic point contact. The effect is due to a relative change of a number of conducting channels when magnetization changes its orientation from parallel to antiparallel.[9] Some attempts were undertaken to measure magnetoresistance through multi-walled carbon nanotubes (MWNT) connected with cobalt electrodes.[10] Although the minimal resistance $R_{min} \approx 9\mathrm{k}\Omega$ was less than the resistance quantum $R_Q = 13\mathrm{k}\Omega$ typical for the ballistic transport, the magnetoresistance was rather low $MR \approx 0.02$. One could not distinguish any

mechanism of the magnetoresistance from these experimental data[10]; moreover there was lack of any features of interference, which were well seen for SWNTs connected to the gold electrodes[6].

The purpose of the present work is to study the coherent electronic transport between ferromagnetic electrodes separated by a nonmagnetic nanoparticle (e.g. either a quantum dot or a molecule). The electrodes are assumed to be in the form of thin films with an in-plane magnetization perpendicular to the direction of the current flow. For a nanoscopic gap between the electrodes, the stray magnetic fields at the particle vanish. In considerations we take into account Coulomb interactions at the particle with special attention on the correlations between electrons with opposite spin orientations flowing through the particle. The considered system is of a transistor type with a gate electrode, which allows to shift a position of the energy level and to change a number of electrons at the particle. We expect for the deep dot level the Kondo resonance with a peak in a local density of states at the Fermi energy, what reflects a formation of a singlet state. Passing from the Kondo regime to the empty state regime one can observe a crossover from the strongly correlated to the uncorrelated electron system. It is of a special interest to examine whether the singlet state in the Kondo regime is preserved with increasing polarization of electrodes.

The paper is organized as follows: In section 2 the model is described and the current is expressed by means of nonequilibrium Green functions. In order to find the Green functions we use (in section 3) the slave-boson method within the mean-field approximation (SBMFA),[11,12] which takes into account essential electronic correlations and captures the Kondo resonance. This method is very simple and efficient for the study of electronic transport in nanostructures,[13] however, it has some limitations. Therefore, in the section 4 we apply the equation of motion method (EOM)[7,14] and compare the results with those obtained within the SBMFA. In the section 5 some final remarks will be given.

II. DESCRIPTION OF THE MODEL AND DETERMINATION OF THE CURRENT

The Hamiltonian for the system with two ferromagnetic electrodes separated by the metallic nanoparticle can be expressed as

$$H = \sum_{k,\alpha,\sigma} \epsilon_{k\alpha\sigma}\, c^{\dagger}_{k\alpha,\sigma} c_{k\alpha,\sigma} + \sum_{\sigma} \epsilon_0\, c^{\dagger}_{0\sigma} c_{0\sigma} + U n_{0\uparrow} n_{0\downarrow} + \sum_{k,\alpha,\sigma} t_{\alpha}\, (c^{\dagger}_{k\alpha,\sigma} c_{0\sigma} + h.c.)\,. \tag{1}$$

The first term describes electrons in the left ($\alpha = L$) and the right ($\alpha = R$) ferromagnetic electrode, the second and the third one correspond to electrons at the particle with the single energy level ϵ_0 and the onsite Coulomb interaction U of two electrons with the opposite spins $\sigma =\uparrow$ and $\sigma =\downarrow$, the fourth term describes tunnelling between the electrodes and the particle.

The current is calculated from the time evolution of the occupation number $\hat{N}_L = \sum_{k,\sigma} c^{\dagger}_{kL,\sigma} c_{kL,\sigma}$ for electrons in the left electrode

$$J \equiv -e\langle \frac{d\hat{N}_L}{dt} \rangle = \frac{ie}{\hbar} [\sum_{k,\sigma} t_L \langle c^{\dagger}_{kL,\sigma} c_{0\sigma} \rangle - c.c.]\,. \tag{2}$$

The thermal averages are expressed by the lesser Green function[15] as

$$\langle c^{\dagger}_{k\alpha,\sigma} c_{0\sigma} \rangle = \int \frac{d\omega}{2\pi i} G^{<}_{0\sigma,k\alpha\sigma}(\omega)\,. \tag{3}$$

From the Dyson equation we find

$$G^{<}_{0\sigma,k\alpha\sigma}(\omega) = t_{\alpha}[g^{r}_{k\alpha\sigma}(\omega) G^{<}_{0\sigma,0\sigma}(\omega) + g^{<}_{k\alpha\sigma}(\omega) G^{a}_{0\sigma,0\sigma}(\omega)]\,, \tag{4}$$

where $g_{k\alpha\sigma}$ is the bare Green function for electrons in the α-electrode, $G_{0\sigma,0\sigma}$ is the dressed Green function at the particle, and the superscript r, a and $<$ denotes the retarded, the advanced and the lesser Green function, respectively. Assuming quasi-elastic transport, for which the current conservation rule is fulfilled for any energy ω, one gets

$$G^{<}_{0\sigma,0\sigma}(\omega) = -2i\mathrm{Im}[G^{r}_{0\sigma,0\sigma}(\omega)][\gamma_{L\sigma} f_L(\omega) + \gamma_{R\sigma} f_R(\omega)], \tag{5}$$

where $\gamma_{\alpha\sigma} = \Gamma_{\alpha\sigma}/\Delta_{\sigma}$, $\Gamma_{\alpha\sigma} = \pi \rho_{\alpha\sigma} t^2_{\alpha}$ and $\Delta_{\sigma} = \Gamma_{L\sigma} + \Gamma_{R\sigma}$. We used the relations for the bare Green functions in the electrodes $g_{\alpha\sigma} = \sum_k g_{k\alpha\sigma} \equiv \sum_k \frac{1}{\omega - \epsilon_{k\alpha\sigma}}$, $g^{<}_{\alpha\sigma} = 2i\pi \rho_{\alpha\sigma} f_{\alpha}$

and $g^{r,a}_{\alpha\sigma} = \mp i\pi\rho_{\alpha\sigma}$, where $\rho_{\alpha\sigma} = 1/(2D_{\alpha\sigma})$ is the assumed constant density of states for $|\epsilon| < D_{\alpha\sigma}$, $D_{\alpha\sigma}$ is a half of the bandwidth and f_α denotes the Fermi distribution function for electrons in the α-electrode. Putting (5) into Eq. (4), (3) and (2) one gets

$$J = \frac{e}{\hbar}\sum_\sigma \frac{2\Gamma_{L\sigma}\Gamma_{R\sigma}}{\Delta_\sigma}\left(\langle n_{R\sigma}\rangle - \langle n_{L\sigma}\rangle\right) , \tag{6}$$

where

$$\langle n_{\alpha\sigma}\rangle = -\frac{1}{\pi}\int_{-D_{\alpha\sigma}}^{D_{\alpha\sigma}} d\omega f_\alpha(\omega)\mathrm{Im}[G^r_{0\sigma,0\sigma}(\omega)] . \tag{7}$$

The charge and the spin accumulation at the particle are expressed as $\langle n_0\rangle \equiv \sum_\sigma \langle n_{0\sigma}\rangle = \sum_{\alpha,\sigma}\gamma_{\alpha\sigma}\langle n_{\alpha\sigma}\rangle$ and $\langle m_0\rangle \equiv \sum_\sigma \sigma\langle n_{0\sigma}\rangle = \sum_{\alpha,\sigma}\sigma\gamma_{\alpha\sigma}\langle n_{\alpha\sigma}\rangle$, respectively. There are several possible choices for treatment of electronic correlations and calculation of the Green function $G^r_{0\sigma,0\sigma}$. We choose the slave-boson approach well adopted to describe the Kondo regime and complement the calculations by the equation of motion treatment, which allows to get a deeper insight into the mixed valence range.

III. SLAVE-BOSON APPROACH

Slave-boson fields were used for decades in strongly correlated electron systems (see [16] for a review). In the context of the Anderson model of a magnetic impurity, the slave-boson representation was first used by Barnes[11] and later developed by Coleman[12] and others[17]. Within this approach the annihilation operator $c_{0\sigma}$ of an electron at the particle is expressed in terms of the slave-boson operators e_0, d_0 and the slave-fermion operator $f_{0\sigma}$

$$c_{0\sigma} = e_0^\dagger f_{0\sigma} + \sigma f_{0\sigma}^\dagger d_0 . \tag{8}$$

The local eigenstates $|0\rangle$, $|\sigma\rangle$ and $|2\rangle$ (corresponding to the empty, the single and the doubly occupied state at the particle) are constructed by the auxiliary operators

$$|0\rangle = e_0^\dagger|vac\rangle , \ |\sigma\rangle = f_{0\sigma}^\dagger|vac\rangle , \ |2\rangle = d_0^\dagger|vac\rangle \tag{9}$$

from the vacuum state $|vac\rangle$. In order to operate in the physical space the auxiliary operators should obey the constraint

$$e_0^\dagger e_0 + \sum_\sigma f_{0\sigma}^\dagger f_{0\sigma} + d_0^\dagger d_0 = 1 . \tag{10}$$

The slave-boson representation (8) gives the reliable results for the equilibrium situation and for the system with paramagnetic electrodes. It is well known[12,17,18] that this representation can be generalized for large spin degeneracy N. The mean-field approximation gives then exact results in the limit $N \to \infty$ and $T = 0$. Moreover, one can include Gaussian fluctuations about mean field solution, which corresponds to the $1/N$ corrections. The local density of states shows then two peaks corresponding to the charge and the spin fluctuations, respectively.

Kotliar and Ruckenstein[19] proposed other approach using four slave-boson operators for representation of the electron operator $c_{0\sigma}$. The method is associated with the Guzwiller approximation and has been widely used in the last decade for studies of the ground state of strongly correlated electrons in lattice models.[16] For the Anderson model of a single–magnetic impurity this approach gives, however, a mean-field stable solution with the local magnetic moment ($\langle n_{0\uparrow}\rangle \neq \langle n_{0\downarrow}\rangle$) for large U and $T = 0$ (for paramagnetic electrodes), in contrast to the exact solution $\langle n_{0\uparrow}\rangle = \langle n_{0\downarrow}\rangle$.

We choose the Barnes-Coleman representation (8) for studies of our model with the ferromagnetic electrodes, because this method gives the reliable results for the paramagnetic case and describes a continuous evolution of physical quantities when the magnetization in the electrodes increases. We are aware that within the mean field approximation (MFA) the method takes into account spin fluctuations but neglects charge fluctuations. The one particle Green function has the quasi-particle contribution only. In order to get the full electronic spectrum one has to include the 1/N corrections (see for example [12] and the chapter 8 in [18]). Moreover, the Barnes-Coleman representation by its construction underestimates long range spin correlations, which may eventually lead to magnetic solutions for the electrodes with a very high magnetic polarization.

The expression (8) is introduced into the Hamiltonian (1). In order to find the Green functions we use the mean-field approximation, within which the slave-boson operators are treated as the complex numbers. Moreover, it is assumed $U \to \infty$, in which the double occupancy at the particle is prohibited ($d_0 = 0$). The problem is reduced then formally to the free electron model with the renormalized parameters $\tilde{t}_\alpha = e_0 t_\alpha$ and $\tilde{\epsilon}_0 = \epsilon_0 + \lambda$, for

the coupling between the electrodes and the particle and the local energy level, respectively. Here, λ denotes the Lagrangian multiplier corresponding to the constraint (10). The stable solution is found from the saddle point of the partition function, i.e., from the minimum of the free energy with respect to the variables e_0 and λ. The free energy is the sum of the fermionic and the bosonic parts $F = F_f + F_b$, which are given by

$$F_f = -\sum_{\alpha,\sigma} \mathrm{Im} \int_{-D_{\alpha\sigma}}^{D_{\alpha\sigma}} \frac{d\omega}{2\pi D_{\alpha\sigma}} f_\alpha(\omega) \ln(\xi_\sigma - \omega), \tag{11}$$

$$F_b = \lambda(e_0^2 - 1). \tag{12}$$

Here, $\xi_\sigma = \tilde{\epsilon_0} + i\tilde{\Delta}_\sigma$ and $\tilde{\Delta}_\sigma = e_0^2 \Delta_\sigma$. The minimum of F is determined by

$$\frac{\partial F}{\partial \lambda} = \frac{\partial F_f}{\partial \lambda} + (e_0^2 - 1) = 0, \tag{13}$$

$$\frac{\partial F}{\partial e_0} = \frac{\partial F_f}{\partial e_0} + \lambda e_0 = 0. \tag{14}$$

These equations can be expressed in the form

$$1 - e_0^2 = \sum_{\alpha,\sigma} \gamma_{\alpha,\sigma} \mathrm{Im}[A_{\alpha,\sigma}] \ , \tag{15}$$

$$\lambda = 2 \sum_{\alpha,\sigma} \Gamma_{\alpha,\sigma} \mathrm{Re}[A_{\alpha,\sigma}] \ , \tag{16}$$

where

$$A_{\alpha,\sigma} = -\frac{1}{\pi} \int_{-D_{\alpha\sigma}}^{D_{\alpha\sigma}} d\omega f_\alpha(\omega) \tilde{G}^r_{0\sigma,0\sigma}(\omega) \tag{17}$$

and the Green functions $\tilde{G}^r_{0\sigma,0\sigma}$ is given by

$$\tilde{G}^r_{0\sigma,0\sigma}(\omega) = \frac{1}{\omega - \tilde{\epsilon_0} + i\tilde{\Delta}_\sigma} \ . \tag{18}$$

The equation (15) is the condition for the average number of electrons at the particle and the equation (16) gives the shift of the resonant level. In the SBMFA the local density of states has a Lorentzian peak close to the Fermi energy (at $\tilde{\epsilon}_0$), with the renormalized width $\tilde{\Delta}_\sigma$. The method ignores the charge fluctuations and consequently no peak occurs in the density of state at ϵ_0.

Let us analyze the situation for the small voltage $V \to 0$ and the temperature $T = 0$. The conductance is calculated from

$$\mathcal{G} = \frac{e^2}{h} \sum_\sigma \frac{4 e_0^2 \Gamma_{L\sigma} \Gamma_{R\sigma}}{\tilde{\epsilon}_0^2 + \tilde{\Delta}_\sigma^2} = \frac{e^2}{h} \sum_\sigma 4 \gamma_{L\sigma} \gamma_{R\sigma} \sin^2(\pi \langle n_{0\sigma} \rangle) \ , \tag{19}$$

where $\langle n_0 \rangle$ and λ are determined from the set of self-consistent equations (15)-(16). Fig.1a presents the conductance as a function of the position of the particle energy level $\epsilon_0 - \epsilon_F$ (with respect to the position of the Fermi level taken as $\epsilon_F = 0$) for the parallel $\mathcal{G}_P$ and the antiparallel $\mathcal{G}_{\mathcal{AP}}$ orientation of magnetization in the electrodes. In the calculations we assumed the density of states in the electrodes $\rho_{L\uparrow} = \rho_{R\uparrow} = 1$ and $\rho_{L\downarrow} = \rho_{R\downarrow} = 1/2$ (i.e. $D_{L\uparrow} = D_{R\uparrow} = 1/2$, $D_{L\downarrow} = D_{R\downarrow} = 1$) for the parallel configuration and $\rho_{L\uparrow} = \rho_{R\downarrow} = 1$ and $\rho_{L\downarrow} = \rho_{R\uparrow} = 1/2$ for the antiparallel configuration. Following the Julliere approach[20] one can express the polarization as $P_\alpha = (\rho_{\alpha\uparrow} - \rho_{\alpha\downarrow})/(\rho_{\alpha\uparrow} + \rho_{\alpha\downarrow})$, which in our case is $P_L = P_R = 1/3$. In the following the limit of strong polarization $P_\alpha \to 1$ is not considered, because it corresponds to the case of vanishing bandwidth of one of spin subbands and it breaks down our assumption on the weak coupling, in which $\Gamma_{\alpha\sigma} \ll D_{\alpha\sigma}$.

The magnetoresistance $MR = (\mathcal{G}_{\mathcal{P}} - \mathcal{G}_{\mathcal{AP}})/\mathcal{G}_{\mathcal{P}}$ is presented in Fig.1b. In the regime of the empty state (for $\tilde{\epsilon}_0 \gg \Delta_\sigma$) one can find

$$MR = \frac{2P_L P_R}{1 + P_L P_R} \, . \tag{20}$$

It is the Julliere formula[20], as one could expect for the uncorrelated transport of electrons. Note that the magnetoresistance in the empty state regime depends only on polarizations of the electrodes. No quantity specifying the particle or its coupling to the leads enters into the formula (20). In the Kondo regime ($\tilde{\epsilon}_0 \to 0$) the conductance is $\mathcal{G} = (e^2/h) \sum_\sigma 4\gamma_{L\sigma}\gamma_{R\sigma}$. In general, an expression for MR has a complex algebraic form. A simpler form of MR is for the system with equal polarization of the electrodes $P_L = P_R = P$

$$MR = \frac{P^2(1 - 3\alpha^2 + \alpha^2 P^2 + \alpha^4 P^2)}{(1 - \alpha^2 P^2)^2} \, , \tag{21}$$

where $\alpha = (t_L^2 - t_R^2)/(t_L^2 + t_R^2)$ describes asymmetry between the left and the right junction. For a large asymmetry $\alpha \to 1$

$$MR = -\frac{2P_L P_R}{1 - P_L P_R} \, . \tag{22}$$

The magnetoresistance is then negative and its absolute value is larger than in the empty state regime [compare with Eq.(20)].

Fig.1c presents the spin accumulation $\langle m_0 \rangle$ at the particle. When a gate voltage is applied to the particle, the position of ϵ_0 is shifted from the empty state regime to the Kondo regime.

The spin accumulation then increases and achieves its maximal value in the mixed valence regime, next it decreases to zero. Using the formula $\langle n_{0\sigma}\rangle = \frac{1}{\pi}\arctan(\tilde{\Delta_\sigma}/\tilde{\epsilon}_0)$ for the average number of electrons with the spin σ valid at $T = 0$, one can easily derive the following relation linking the magnetization with the occupation of the particle

$$\sin(\pi\langle m_0\rangle) = \frac{\Delta_\uparrow - \Delta_\downarrow}{\Delta_\uparrow + \Delta_\downarrow}\sin(\pi\langle n_0\rangle)\ . \tag{23}$$

It means that in the Kondo regime (i.e. when $\langle n_0\rangle \to 1$) the spin accumulation $\langle m_0\rangle \to 0$ and the system achieves the unitary limit with the singlet state. Although the tunnelling rates $\Gamma_{\alpha\sigma}$ are different for electrons with the opposite spin orientation, the Kondo resonance leads to an equal probability to find an electron with the spin $\sigma =\uparrow$ and $\sigma =\downarrow$. The vanishing spin accumulation at the nanoparticle in the Kondo regime is independent on the asymmetry of the junctions (Fig.1c). It is not true for the transmission, where equal values for both spin channels are only achieved for the symmetric case ($t_L = t_R$, $P_L = P_R$). This fact is illustrated in Fig.1a, where for the asymmetric junctions ($t_L \neq t_R$) the conduction does not reach the maximal value $2e^2/h$ in the Kondo limit. Qualitatively similar behavior (not presented) holds for for $t_L = t_R$ but $P_L \neq P_R$.

The relation (23) is valid for free electrons ($U = 0$) as well. There is a difference in the dependence of the average number of electrons $\langle n_0\rangle$ on the position of the particle level ϵ_0, which for the correlated electrons within the SBMFA is expressed by the renormalized value $\tilde{\epsilon}_0 = \epsilon_0 + \lambda$. Using the electron-hole symmetry in our model (1) one finds that in the limits $\langle n_0\rangle \to 0$ and $\langle n_0\rangle \to 2$ electronic correlations are irrelevant and the magnetoresistance is the same as for free electrons. The absolute value of $\langle m_0\rangle$ is equal in both the limits, but its sign is opposite. Therefore, we expect that $\langle m_0\rangle = 0$ for the symmetric Anderson model with ferromagnetic electrodes, i.e. when $\epsilon_0 = U/2$ and $\langle n_0\rangle = 1$. The problem shall be undertaken in the next section within the equation of motion approach.

Fig.2 shows the temperature dependence of the conductance and the slave-boson field e_0^2. In the Kondo regime $\mathcal{G}$ and e_0^2 decreases to zero when $T \to T_c$. The sharp transition from the broken symmetry state to the state with vanishing boson field expectation value is an artifact of the MFA. The peak in the density of states disappears at T_c. In the mixed valence regime

the value of T_c is much larger and one can observe an increase of $\mathcal{G}$ corresponding to smearing of the Fermi distribution function (see the curves in Fig.2 corresponding to $\epsilon_0 = 0$). The SBMFA is reliable in the Fermi liquid regime when the temperature T is much lower than the Kondo temperature T_K. Moreover, the method neglects charge fluctuations relevant in the mixed valence regime and at higher temperatures. Therefore, in the next section, we complement the studies of electronic transport by the equation of motion approach.

IV. EQUATION OF MOTION APPROACH

Lets us first describe the equation of motion (EOM) method. The equation for $G^r_{0\sigma,0\sigma}$ at the particle

$$(\omega - \epsilon_0 + i\Delta_\sigma)G^r_{0\sigma,0\sigma}(\omega) = 1 + U\langle\langle c_{0\sigma}c^\dagger_{0\bar{\sigma}}c_{0\bar{\sigma}}|c^\dagger_{0\sigma}\rangle\rangle^r_\omega \,, \tag{24}$$

generates the higher-order Green's function $\langle\langle c_{0\sigma}c^\dagger_{0\bar{\sigma}}c_{0\bar{\sigma}}|c^\dagger_{0\sigma}\rangle\rangle^r_\omega$. Here, $\bar{\sigma}$ denotes the spin orientation opposite to σ. Next, the equation of motion for this function is written

$$(\omega - \epsilon_0 - U)\langle\langle c_{0\sigma}c^\dagger_{0\bar{\sigma}}c_{0\bar{\sigma}}|c^\dagger_{0\sigma}\rangle\rangle^r_\omega = \langle n_{0\bar{\sigma}}\rangle + \sum_{k,\alpha} t_\alpha \Big[\langle\langle c_{k\alpha\sigma}c^\dagger_{0\bar{\sigma}}c_{0\bar{\sigma}}|c^\dagger_{0\sigma}\rangle\rangle^r_\omega - \langle\langle c_{0\sigma}c^\dagger_{k\alpha\bar{\sigma}}c_{0\bar{\sigma}}|c^\dagger_{0\sigma}\rangle\rangle^r_\omega + \langle\langle c_{0\sigma}c^\dagger_{0\bar{\sigma}}c_{k\alpha\bar{\sigma}}|c^\dagger_{0\sigma}\rangle\rangle^r_\omega\Big] \,. \tag{25}$$

We proceed a step further and truncate the series of hierarchy of equations of motions using the self-consistent decoupling procedure proposed by Lacroix[14], within which

$$\langle\langle c_{k\alpha\sigma}c^\dagger_{k'\alpha'\bar{\sigma}}c_{0\bar{\sigma}}|c^\dagger_{0\sigma}\rangle\rangle^r_\omega \approx \langle c^\dagger_{k'\alpha'\bar{\sigma}}c_{0\bar{\sigma}}\rangle G^r_{k\alpha\sigma,0\sigma}(\omega) \,, \tag{26}$$

$$\langle\langle c_{k\alpha\sigma}c^\dagger_{0\bar{\sigma}}c_{k'\alpha'\bar{\sigma}}|c^\dagger_{0\sigma}\rangle\rangle^r_\omega \approx \langle c^\dagger_{0\bar{\sigma}}c_{k'\alpha'\bar{\sigma}}\rangle G^r_{k\alpha\sigma,0\sigma}(\omega) \,, \tag{27}$$

$$\langle\langle c_{0\sigma}c^\dagger_{k\alpha\bar{\sigma}}c_{k'\alpha'\bar{\sigma}}|c^\dagger_{0\sigma}\rangle\rangle^r_\omega \approx \langle c^\dagger_{k\alpha\bar{\sigma}}c_{k'\alpha'\bar{\sigma}}\rangle G^r_{0\sigma,0\sigma}(\omega) \,. \tag{28}$$

The Green's functions from the left hand side of (25) can be written as $\sum_k\langle\langle c_{k\alpha\sigma}c^\dagger_{0\bar{\sigma}}c_{0\bar{\sigma}}|c^\dagger_{0\sigma}\rangle\rangle^r_\omega \approx t_\alpha g^r_{\alpha\sigma}\langle\langle c_{0\sigma}c^\dagger_{0\bar{\sigma}}c_{0\bar{\sigma}}|c^\dagger_{0\sigma}\rangle\rangle^r_\omega$ and

$$\sum_k\langle\langle c_{0\sigma}c^\dagger_{0\bar{\sigma}}c_{k\alpha\bar{\sigma}}|c^\dagger_{0\sigma}\rangle\rangle^r_\omega \approx R_{0\bar{\sigma},\alpha\bar{\sigma}}(\omega) + t_\alpha g^r_{\alpha\bar{\sigma}}\langle\langle c_{0\sigma}c^\dagger_{0\bar{\sigma}}c_{0\bar{\sigma}}|c^\dagger_{0\sigma}\rangle\rangle^r_\omega + R_{0\bar{\sigma},\alpha\bar{\sigma}}(\omega)\sum_{k',\alpha'} t_{\alpha'}G^r_{k'\alpha'\sigma,0\sigma}(\omega) - G^r_{0\sigma,0\sigma}(\omega)\sum_{\alpha'} t_{\alpha'}R_{\alpha'\bar{\sigma},\alpha\bar{\sigma}}(\omega) \,, \tag{29}$$

where $R_{0\bar{\sigma},\alpha\bar{\sigma}}(\omega) = \sum_k \frac{\langle c^\dagger_{0\bar{\sigma}} c_{k\alpha\bar{\sigma}}\rangle}{\omega-\epsilon_{k\alpha\sigma}}$, $R_{\alpha'\bar{\sigma},\alpha\bar{\sigma}}(\omega) = \sum_{k,k'} \frac{\langle c^\dagger_{k'\alpha'\bar{\sigma}} c_{k\alpha\bar{\sigma}}\rangle}{\omega-\epsilon_{k\alpha\sigma}}$. The function $\langle\langle c_{0\sigma} c^\dagger_{k\alpha\bar{\sigma}} c_{0\bar{\sigma}} | c^\dagger_{0\sigma}\rangle\rangle^r_\omega \propto 1/U$ and can be neglected in the limit $U \to \infty$. After these approximations one gets (for $U \to \infty$)

$$G^r_{0\sigma,0\sigma}(\omega) = \frac{1 - \langle n_{0\bar{\sigma}}\rangle + H_{\bar{\sigma}}(\omega)}{\omega - \epsilon_0 + i\Delta_\sigma + i2\Delta_0 H_{\bar{\sigma}}(\omega) + F_{\bar{\sigma}}(\omega)} , \tag{30}$$

where $2\Delta_0 = \Delta_\uparrow + \Delta_\downarrow$,

$$H_{\bar{\sigma}}(\omega) = \sum_\alpha \Gamma_{\alpha\bar{\sigma}} \int \frac{d\omega'}{\pi} \frac{f_\alpha(\omega') G^a_{0\bar{\sigma},0\bar{\sigma}}(\omega')}{\omega' - \omega - i0^+} , \tag{31}$$

$$F_{\bar{\sigma}}(\omega) = \sum_\alpha \Gamma_{\alpha\bar{\sigma}} \int \frac{d\omega'}{\pi} \frac{f_\alpha(\omega')}{\omega' - \omega - i0^+} =$$

$$\sum_\alpha \frac{\Gamma_{\alpha\bar{\sigma}}}{\pi} \Big\{ i\pi f_\alpha(\omega) + \ln \frac{2\pi k_B T}{D_{\alpha\bar{\sigma}}} + \mathrm{Re}\Psi\Big[\frac{1}{2} - i\frac{\omega - \epsilon_{F\alpha}}{2\pi k_B T}\Big]\Big\} . \tag{32}$$

Here, $\mathrm{Re}\Psi$ denotes the real part of the digamma function and $\epsilon_{F\alpha}$ is the position of the Fermi level in the α electrode. Eqs.(30)-(31) and the condition

$$\langle n_{0\sigma}\rangle = -\frac{1}{\pi} \sum_\alpha \int_{-D_{\alpha\sigma}}^{D_{\alpha\sigma}} d\omega\ \gamma_{\alpha\sigma} f_\alpha(\omega) \mathrm{Im}[G^r_{0\sigma,0\sigma}(\omega)] \tag{33}$$

consist a set of self-consistent integral equations, which have to be solved.

At $T = 0$ the function $H_{\bar{\sigma}}(\omega)$ and $F_{\bar{\sigma}}(\omega)$ has a logarithmic singularity at the Fermi level $\omega = \epsilon_{F\alpha}$, but $G^r_{0\sigma,0\sigma0}(\omega)$ varies more smoothly around this point. At the equilibrium the equation (30) for the Green function can be written as

$$G^r_{0\sigma,0\sigma}(\epsilon_F) = \frac{G^a_{0\bar{\sigma},0\bar{\sigma}}(\epsilon_F)}{i2\Delta_0 G^a_{0\bar{\sigma},0\bar{\sigma}}(\epsilon_F) + 1} . \tag{34}$$

Assuming the solution in a form $G^r_{0\sigma,0\sigma}(\epsilon_F) = [1 - e^{2i\phi_\sigma}]/(2i\Delta_\sigma)$ one gets

$$\sin(\phi_\uparrow - \phi_\downarrow) = \frac{\Delta_\uparrow - \Delta_\downarrow}{\Delta_\uparrow + \Delta_\downarrow} \sin(\phi_\uparrow + \phi_\downarrow) . \tag{35}$$

Taking the phase shift $\phi = \phi_\uparrow + \phi_\downarrow$ according to the Friedel sum rule $\phi = \pi\langle n_0\rangle$ and $\eta = \phi_\uparrow - \phi_\downarrow = \pi\langle m_0\rangle$ the relation (35) becomes the same as the one (23) derived for the SBMFA. Again we come to the conclusion that the spin accumulation $\langle m_0\rangle \to 0$ in the Kondo regime.

In general, the Green function $G^r_{0\sigma,0\sigma}(\omega)$ was determined numerically solving the set of Eqs.(30)-(33). The singularity at ϵ_F was treated with a special care. Integration around

the singularity point was performed according to a logarithmic discretization procedure[18]. In Fig.3 the density of states (DOS) is presented for both spin orientations. Besides the sharp Kondo peak close to $\epsilon_F = 0$, one can see the broad peak close to ϵ_0 corresponding to charge fluctuations. Since the real part of the denominator of the Green function (30) is different for both spin orientations, the maxima of the charge fluctuations peaks are at different positions. Moreover, one can see that the weight of DOS for $\sigma =\uparrow$ is much larger than that for $\sigma =\downarrow$. This results from the nominator of $G^r_{0\sigma,0\sigma}$ (30), which is different for the opposite spin directions. It is in contrast to the SBMFA, where no spin asymmetry of the weights is observed – compare the Green functions (30) and (18). The difference reflects the fact that the SBMFA solution (18) completely neglects charge fluctuations.

Fig.4a presents the conductance $\mathcal{G}_P$ and $\mathcal{G}_{AP}$ for the parallel and the antiparallel configuration of the magnetization (solid and dashed curves, respectively). It is seen that with lowering of the temperature the peak of $\mathcal{G}$ is shifted (as expected [21]) to the Kondo regime.

The magnetoresistance is presented in Fig.4b. In the empty state regime it is similar to the SBMFA result (compare Fig.1b). In the mixed valence regime MR behaves different, it increases and achieves large values. Moreover, MR shows a strong temperature dependence. In this range the contribution of the charge fluctuations is dominant and since the width of the peaks of the DOS for the opposite spin directions are different, so the different temperature dependence of the conductance results. A further shift of ϵ_0 into the Kondo regime leads to a reduction of MR, which achieves its minimal value given by Eq.(21) (for our case $MR = P^2 = 1/9$).

The spin accumulation $\langle m_0 \rangle$ calculated within the EOM approach (Fig.4c) is much larger than that for the SBMFA (compare Fig.1c). Its maximal value can be as large as 0.8 at $\epsilon_0 \approx -0.02$, which means that electrons with the spin $\sigma =\uparrow$ are mostly transferred through the particle. In the Kondo regime we recover the SBMFA result with $\langle m_0 \rangle \to 0$. It is weakly temperature dependent (in contrast to $\mathcal{G}$ and MR). For the antiparallel configuration there is no spin accumulation for any ϵ_0 (see the dashed curve in Fig.4c). It results from the transfer rates to and from the particle, which are equal for both spin orientations in the case of symmetric junctions.

Temperature characteristics of our system are presented in Fig.5 for $\epsilon_0 = -0.025$. The EOM approach[14] gives the Kondo temperature $T_K = 0.57D/k_B \exp[-\pi(\epsilon_F - \epsilon_0)/\Delta_0]$, which for our case with $D = D_{L\downarrow} = 1$ is $T_K = 3.5 \times 10^{-5}$. The conductance (presented in Fig.5a) decreases in a very wide temperature range (over four orders of magnitude) and saturates at temperatures $T \approx 10^{-4}$. We drew also a series of auxiliary figures (not presented) with the DOS for various temperatures (similar to Fig.3) and found that the Kondo peak disappeared at $T \approx 10^{-4}$. For higher temperatures the value of $\mathcal{G}$ is connected with the broad peak of the DOS corresponding to the charge fluctuations, which is weakly temperature dependent. The spin accumulation depends on both the peaks, corresponding to the charge and the spin fluctuations. However, the weight of the Kondo peak is small and its contribution to the electron occupation $\langle n_{0\sigma} \rangle$ is small as well. Therefore, $\langle m_0 \rangle$ starts to decrease at a much higher temperature $T \approx \Delta_0/k_B$ (see the Fig5.b), when the charge fluctuation peak becomes to be deformed. Fig.5 shows also that at low temperatures $\mathcal{G}_{AP}$ decreases quicker than $\mathcal{G}_P$, which results in the magnetoresistance increases first, then decrease and finally the value for uncorrelated electronic transport given by Eq.(20) is reached.

V. FINAL REMARKS

In the paper we considered the coherent transport through magnetic nanojunctions separated by a nanoparticle and a role of electronic correlations. In the empty state regime the transport is uncorrelated and the Julliere formula for the magnetoresistance was recovered. We showed that in the Kondo regime the conductance reaches the unitary limit and the singlet state is formed, for which the spin accumulation reaches zero. Correlations between electrons lower the value of the magnetoresistance, which can be even negative for asymmetric junctions. Analytical formulae were derived for MR in the system with the electrodes of the same polarization as well as in the limit of strong asymmetry between the junctions. The slave-boson mean field approach and the equation of motion method were used in the studies, and both of them gave quantitatively the same results in the Kondo regime and in the empty state regime. For the mixed valence regime we predict a large magnetoresistance,

which should exhibit a strong temperature dependence.

Very recently appeared a paper by Sergueev et al. [22] discussing also the spin polarized transport through a quantum dot. In opposite to our studies they concentrate exclusively on the Kondo regime and the main point of their interest is the contribution of the Kondo resonance to the spin valve effect. Their finding of the singlet Kondo state in the presence of magnetic electrodes is in agreement with our conclusions.

In the presented discussion all the information on correlations of electrons in the electrodes is included in the magnetic polarization only. In this simplified picture the electrodes are treated as two independent reservoirs of spin dependent noninteracting quasiparticles. The source of magnetism in the electrodes is coulomb and exchange interactions, which not only determine the ground state but also the response of the subsystem. This problem has to be studied by many-particle Green functions including vertex corrections. The essential point of such more fundamental approach is that the processes for each spin channel do not proceed separately but the interactions mix the channels. The Kondo resonance at the nanoparticle is caused by collective excitations of the low-energy particle-hole pairs that lead to logarithmic singularities. In the response of the conduction electron subsystem the electron-hole pairs with opposite spins take also part. One can expect that electronic correlations in the electrodes influence of the Kondo resonance and modify the Kondo exchange coupling. This topic has been discussed in serval papers (see e.g. [23,24]) in the context of magnetic impurity in a correlated electron medium in the paramagnetic phase. The studies[23] showed that for the weakly correlated case (with a small onsite coulomb integral $U_\alpha \ll D_\alpha$) spin fluctuations of conduction electrons are enhanced with an increase of U_α, which results in an enhancement of both the Kondo exchange coupling and the Kondo temperature. For the strong coupling between the impurity and the medium ($\Gamma_\alpha \approx D_\alpha$) and the strong correlations of conducting electrons ($U_\alpha > D_\alpha$) the studies[24] suggest that the single Kondo picture leading to logarithmic divergences breaks down even for a paramagnetic medium. The theory is, however, not well developed for this case. Those studies[23,24] support our statement that the Kondo resonance should occur in the system with the magnetic electrodes for the weak coupling between the nanoparticle and the electrodes ($\Gamma_{\alpha\sigma} \ll D_{\alpha\sigma}$) and

for the small polarization ($P_\alpha \ll 1$). The present approach can not be applied in the limit of large polarization ($P_\alpha \to 1$), where one can expect a break-down of the Kondo resonance and magnetic solutions for whole range of ϵ_0.

A ferromagnetic single electron transistor (fSET) has a similar construction[25] to the model discussed in this paper. The tunnel barriers between the electrodes and the nanoparticle are assumed to be thicker in the fSET and therefore, transport is an incoherent sequential tunneling process. The current-voltage (I-V) characteristic shows[25] a Coulomb blockade effect in a low voltage regime. Moreover, for a high voltage the I-V curve is asymmetric like in a diode and the fSET can operate as a spin filter. Electronic correlations at the nanoparticle lead to an increase of the magnetoresistance for the incoherent sequential tunnelling – in contrast to the present results (21)-(22) for the coherent transport.

ACKNOWLEDGMENTS

The work was supported by the State Committee for Scientific Research Republic of Poland under Grant No. 2 P03B 087 19.

REFERENCES

[1] see for example: J. M. Daughton, J. Magn. Magn. Mat. **192**, 334 (1999) and references therein.

[2] see for example: S. Mitani, H. Fujimori, K. Takanashi, K. Yakushiji, J.-G. Ha, S. Takahashi, S. Maekawa, S. Ohnuma, N. Kobayashi, T. Masumoto, M. Ohnuma and K. Hono, J. Magn. Magn. Mat. **192**, 179 (1999) and references therein.

[3] J. Barnaś and A. Fert, Phys. Rev. Lett. **80**, 1058 (1998).

[4] K. Yakushiji, S. Mitani, K. Takanashi, S. Takahashi, S. Maekawa, H. Imamura and H. Fujimori, Appl. Phys. Lett. **78**, 515 (2001).

[5] J. Gores, D. Goldhaber-Gordon, S. Heemeyer, M. A. Kastner, H. Shtrikman, D. Mahalu and U. Meirav, Phys. Rev. B **62**, 2188 (2000).

[6] W. Liang, M. Bockrath, D. Bozovic, J. H. Hafner, M. Tinkham, and H. Park, Nature **411**, 665 (2001); J. Nygard, D. H. Cobden and P. E. Lindelof, Nature **408**, 342 (2000).

[7] B. R. Bułka and P. Stefański, Phys. Rev. Lett. **86**, 5128 (2001).

[8] N. Garcia, M. Munoz and Y.-W. Zhao, Phys. Rev. Lett. **82**, 2923 (1999).

[9] H. Imamura, N. Kobayashi, S. Takahashi and S. Maekawa, Phys. Rev. Lett. **84**, 1003 (2000).

[10] K. Tsukagoshi, B. W. Alphenaar, and H. Ago, Nature **401**, 572 (1999).

[11] S. E. Barnes, J. Phys. F **6**, 1375(1976); **7**, 2637 (1977).

[12] P. Coleman, Phys. Rev. B **29**, 3035 (1984); B **35**, 5072 (1987).

[13] see for example: R. Aguado and D. C. Langreth, Phys. Rev. Lett. **85**, 1946 (2000).

[14] C. Lacroix, J. Phys. F Metal Phys. **11**, 2389 (1981).

[15] For a technique of the nonequilibrium Green functions and its applications in electronic transport, see: H. Haug and A.-P. Jauho, *Quantum Kinetics in Tranport and Optics of Semiconductors*, (Springer Verlag, Berlin Heildelberg New York, 1998); D. K. Ferry, *Transport in nanostructures*, (Cambridge University Press, Cambridge 1997).

[16] R. Frésard and P. Wolfle, Int. J. Mod. Phys. B **6**, 237 (1992); F. Gebhard, *The Mott metal-insulators transition: Models and methods*, (Springer Verlag, Berlin Heildelberg New York, 1997).

[17] N. Read D. Newns, J. Phys. C**16**, 3473 (1983); A. Auerbach, K. Levin, Phys. Rev. Lett. **57**, 877 (1986); Phys. Rev. B **34**, 3524 (1986); M. Lavagna, et al., Phys. Rev. Lett. **58**, 266 (1987); A. J. Millis and P. A. Lee, Phys. Rev. B **35**, 3394 (1987).

[18] A. C. Hewson, *The Kondo problem to heavy fermions* (Cambridge University Press, Cambridge 1993).

[19] G. Kotliar and A. E. Ruckenstein, Phys. Rev. Lett. **57**, 1362 (1986).

[20] M. Julliere, Phys. Lett. **54A**, 225 (1975).

[21] L. I. Glazman and M. E. Raikh, Pis'ma Zh. Eksp. Teor. Fiz. **47**, 378 (1988) [JETP Lett. **47**, 452 (1988)]; T. K. Ng and P. A. Lee, Phys. Rev. Lett. **61**, 1768 (1988); A. Kawabata, J. Phys. Soc. Jpn. **60**, 3222 (1991).

[22] N. Sergueev, Q.-f. Sun, H. Guo, B. G. Wang and J. Wang, Phys. Rev. B **65**, 165303

(2002)

[23] T. Schork and P. Fulde, Phys. Rev. B **50**, 1345 (1994); G. Khaliullin and P. Fulde, Phys. Rev. B **52**, 9514 (1995); T. Schork, Phys. Rev. B **53**, 5626 (1996);.

[24] B. Davidovich and V. Zevin, Phys. Rev. B **57**, 7773 (1998).

[25] B. R. Bulka, Phys. Rev. B **62**, 1186 (2000).

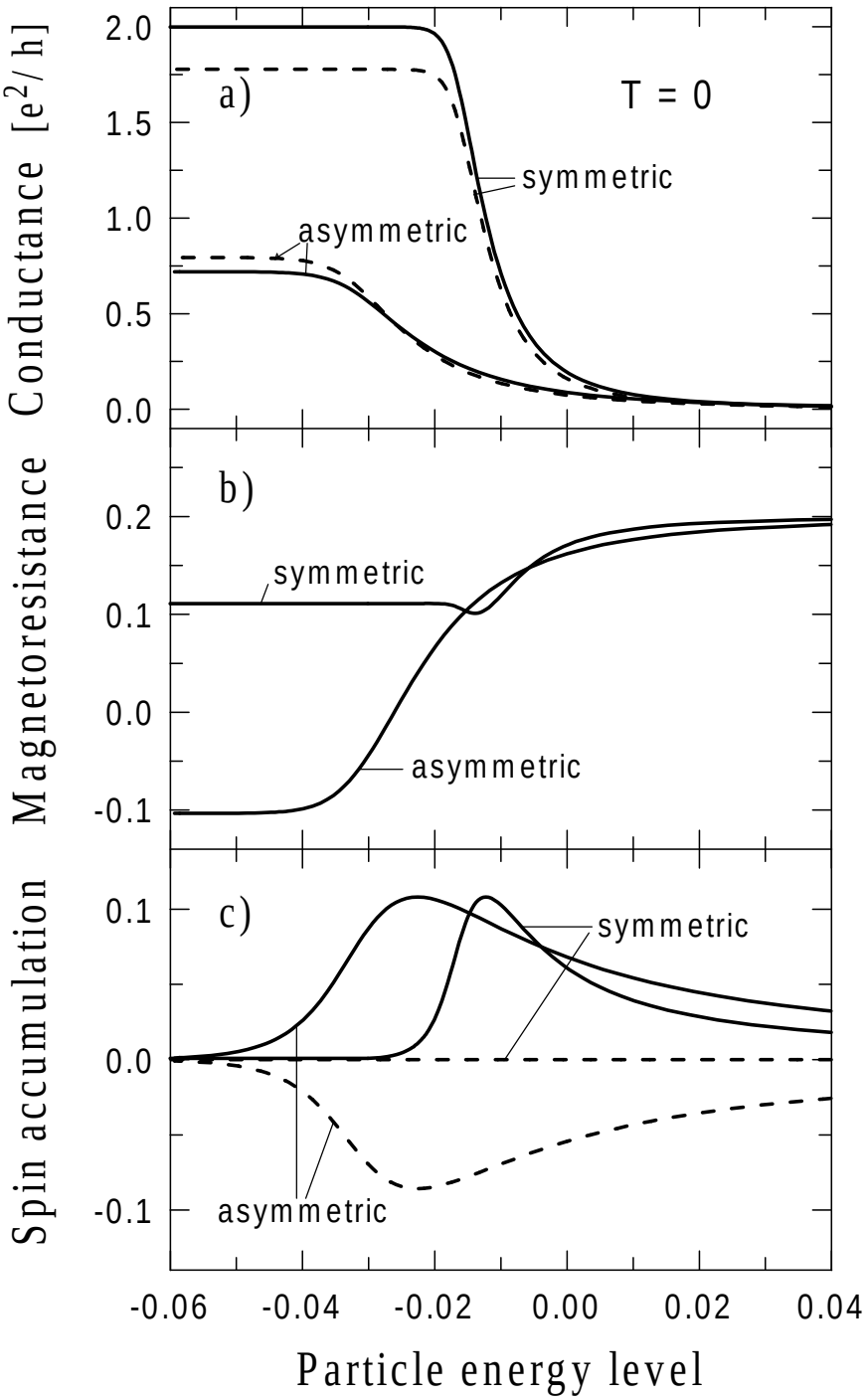

FIG. 1: The results of the SBMFA for the conductance (a), the magnetoresistance (b) and the spin accumulation as a function of the relative position of the energy level $\epsilon_0 - \epsilon_F$ of the particle for the symmetric junction ($t_L = 0.03$, $t_R = 0.03$) and the asymmetric junction ($t_L = 0.02$, $t_R = 0.06$) at the temperature $T = 0$. All parameters are in units of the half-band width $D_{L\downarrow} = 1$. The solid and the dashed curves correspond the situation for the parallel and for the antiparallel orientation of magnetization in the electrodes. The polarization is taken $P_\alpha = 1/3$.

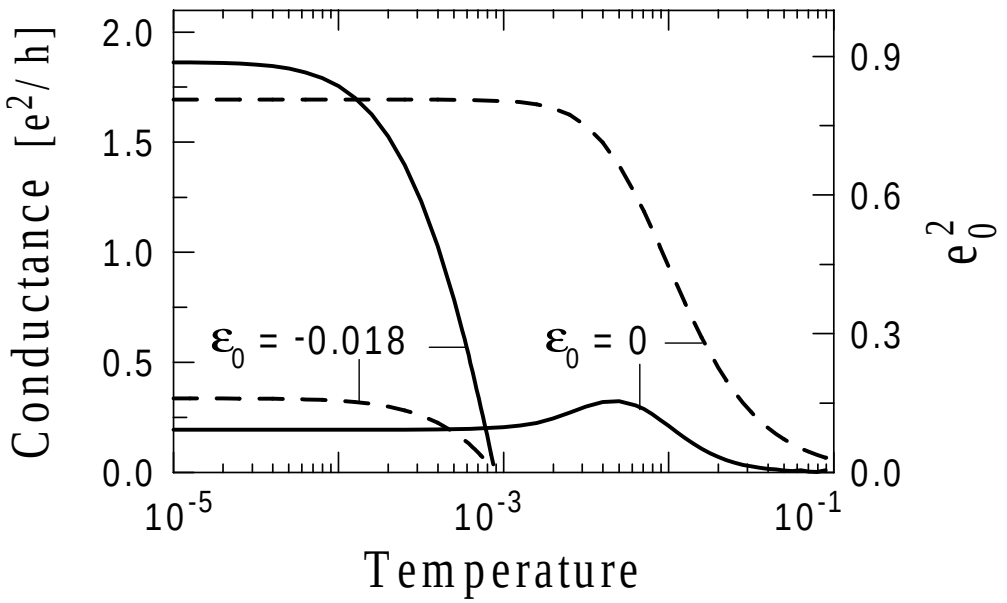

FIG. 2: Temperature dependence of the conductance (solid curve) and the boson occupation parameter e_0^2 (dashed curve) for $\epsilon_0 = -0.018$ and 0. The contacts are symmetric ($t_L = 0.03$, $t_R = 0.03$), the polarizations in the electrodes $P_L = P_R = 1/3$ are oriented parallel.

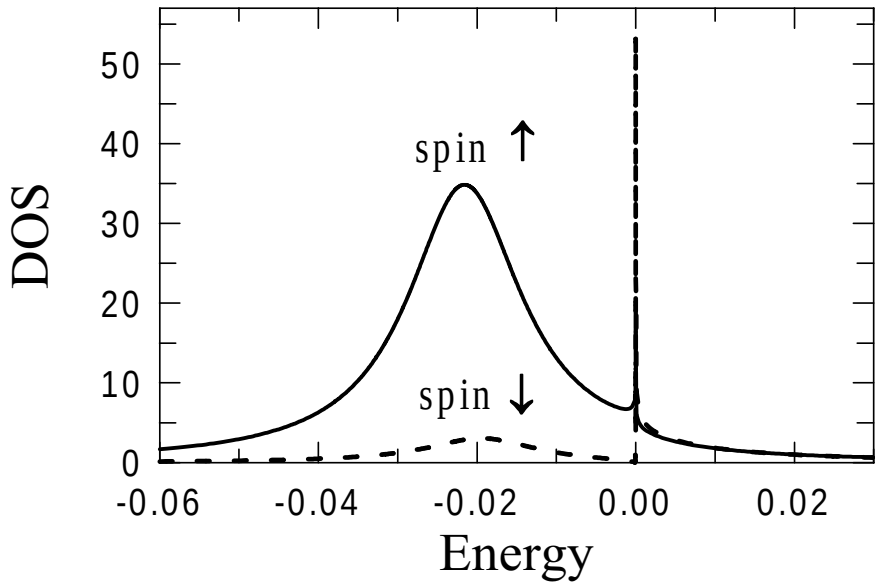

FIG. 3: Local density of states (DOS) determined by the EOM method for the spin orientation $\sigma =\uparrow$ (solid curve) and $\sigma =\downarrow$ (dashed curve) at $T = 10^{-7}$. The parameters are $\epsilon_0 = -0.02$, $t_L = t_R = 0.03$, $\Delta_0 = 0.0085$ and $P_L = P_R = 1/3$.

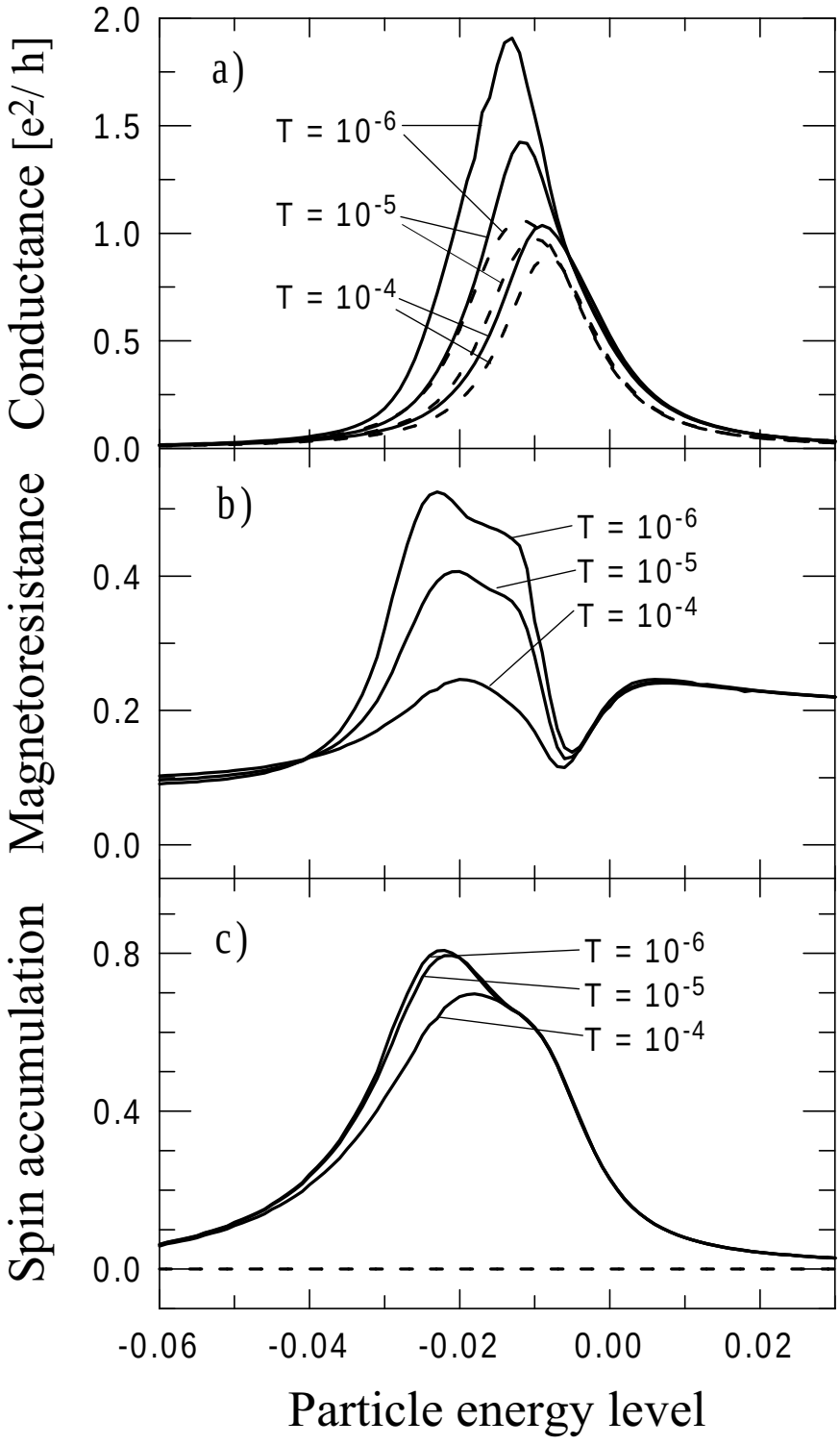

FIG. 4: The conductance (a) calculated by means of the EOM approach for the parallel and the antiparallel orientation of magnetization in the electrodes (solid and dashed curves), the magnetoresistance (b) and the spin accumulation (c) as a function of the position of the dot level for different temperatures $T = 1 \times 10^{-6}$, 1×10^{-5} and 1×10^{-4}. The other parameters are the same as those in Fig.3.

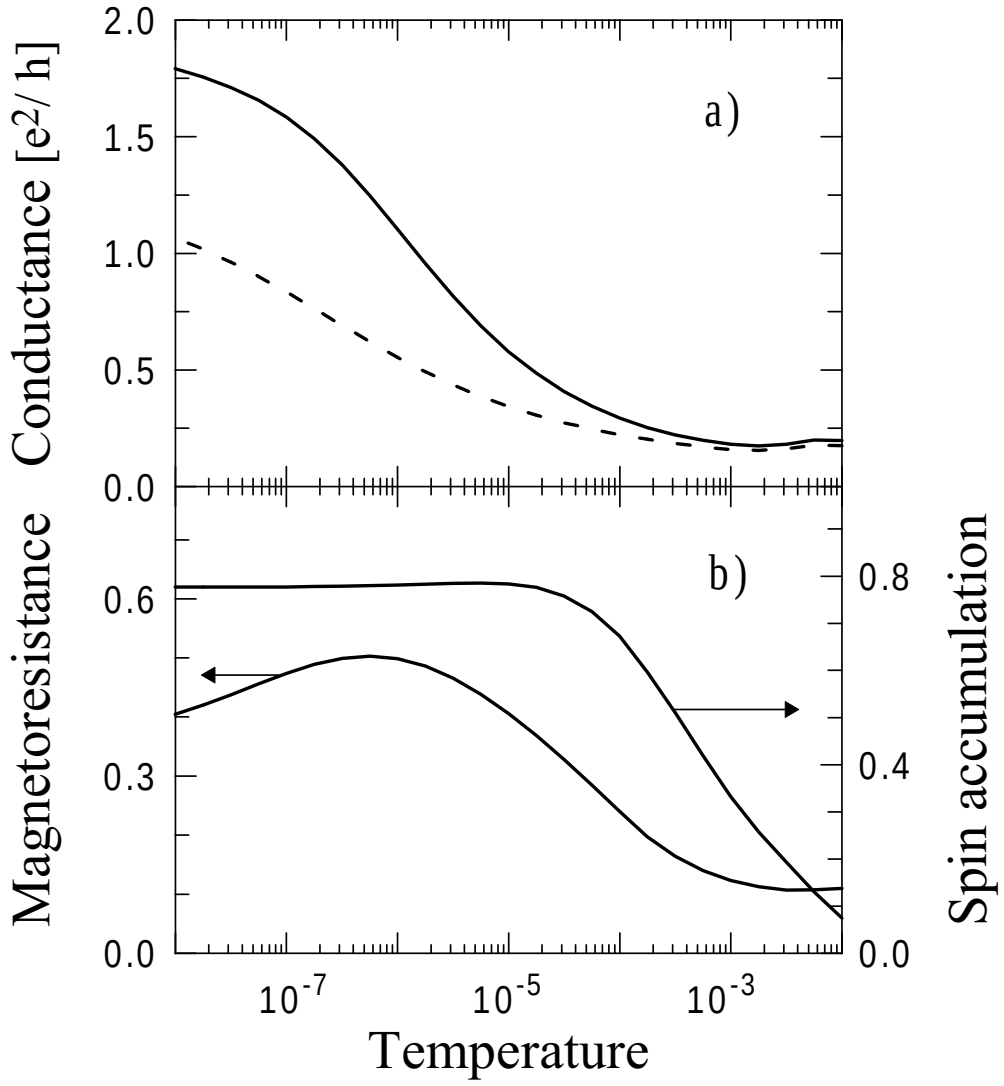

FIG. 5: Temperature dependence of the conductance (a) for the parallel and the antiparallel orientation of magnetization in the electrodes (solid and dashed curves), the magnetoresistance and the spin accumulation (b) for $\epsilon_0 = -0.02$. The Kondo temperature is estimated as $T_K = 3.5 \times 10^{-5}$. The other parameters are the same as those in Fig.3.